Supplemental Materials for Possible Magnetic Structure with a Tilted Helical Plane in $SmBe_{13}$ Probed by ^{9}Be-NMR Study

Hiroyuki Hidaka[1*], Yoshihiko Ihara[1], Tatsuya Yanagisawa[1], and Hiroshi Amitsuka[1]

[1]*Graduate School of Science, Hokkaido University, Sapporo, Hokkaido 060-0810, Japan*

1. Estimation of hyperfine coupling constant

To estimate the anisotropic hyperfine coupling constant of $SmBe_{13}$, we need to understand the ^{9}Be-NMR spectrum. First we will assign the peaks in the Be-NMR spectrum to corresponding Be sites. In the crystal structure of RBe_{13}, Be occupies two crystallographically independent 8*b* site [Be(I)] and 96*i* site [Be(II)]. The NMR spectrum mainly originates from Be(II) sites because of a larger number of nuclei in a unit cell, Be(I):Be(II) = 1:12. The signal from Be(I) site was not identified in this study. Since the electric field gradient (EFG) at Be(II) site is finite because of a low site symmetry, three NMR peaks from m = 3/2 ⇔ 1/2, 1/2 ⇔ -1/2, and -1/2 ⇔ -3/2 transitions will be observed for the ^{9}Be nuclear spins with I = 3/2. Besides, when a magnetic field is applied to [001] direction, the crystallographic three-fold symmetry is magnetically broken, and thus three sets of three-peaks will be observed. The magnetically nonequivalent three sets of peaks are labeled as R, G, and B as shown in Fig. S1(a). We clearly resolved NMR signals from these sites at 60 K because of rather small linewidth as shown in Fig. S1(b). The highly resolved spectrum at 60 K shows a good sample quality and confirms that the external field is aligned parallel to the [001] direction, because even a small misalignment further lowers the local symmetry which results in a significant line broadening. The three sets of Be(II) spectra are decomposed as indicated at the bottom of Fig. S1(b), and the NQR frequencies obtained by the separation of each set of peaks are n_Q = (17, 68, 85) kHz. Similar results were reported for a sister compound UBe_{13}, in which the direction for the smallest NQR frequency is perpendicular to the mirror plane, that is, parallel to the crystalline axis.[SM1)] The other principal axes of EFG in the mirror plane are slightly tilted from the crystalline axes. According to the result for UBe_{13}, we assign these spectra in $SmBe_{13}$ to the crystal structure as represented in Fig. S1(b).

*hidaka@phys.sci.hokudai.ac.jp

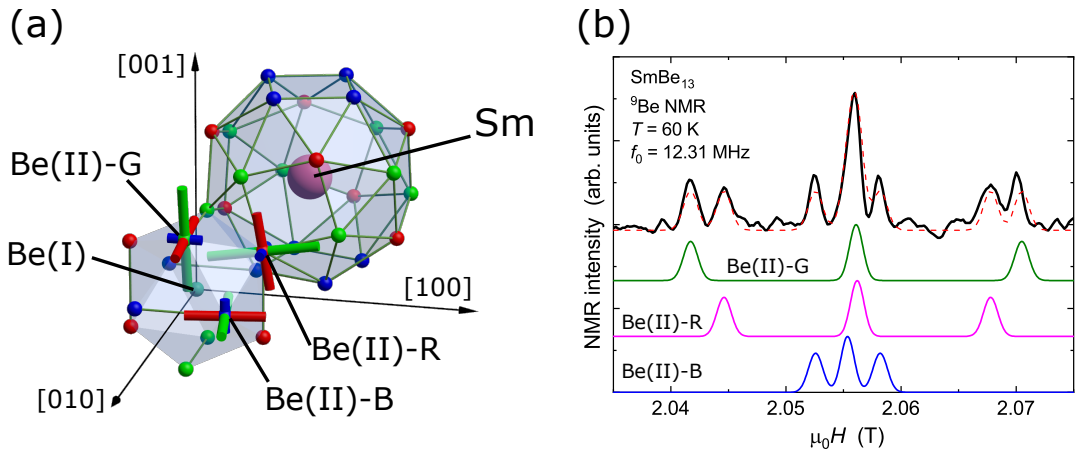

Fig. S1. (Color online) (a) Be(II) sites assigned for three sets of ^{9}Be NMR spectra. EFG principal axes are represented as bars on the Be sites. (b) ^{9}Be NMR spectrum in the field applied parallel to [001] direction at 60 K.

Based on the spectrum assignment described above, we can measure the anisotropic Knight shift for three different field directions with respect to the EFG principal axes at the same time. The temperature dependence of the Knight shift K for each site is shown in Fig. S2. The Knight shift was measured at approximately 5 T for better resolution. The temperature dependence of Knight shift scales to that of the bulk susceptibility $\chi(T)$ above 15 K for all sites.[11)] At lower temperatures the peak positions were not determined precisely because of the spectrum broadening near the magnetic phase transition, where the linewidth becomes comparable to the NQR splitting, as indicated in Fig. 2 of the main text. Within the temperature range between 100 and 15 K, a linear relationship between K and χ was observed as demonstrated by the K–χ plot shown in the inset to Fig. S2. From the slope in the K–χ plot, we obtain the anisotropic hyperfine coupling constants as $A_{\rm hf}$ = 0.33, 0.21, 0.24 T/$\mu_{\rm B}$. This hyperfine coupling constants can be decomposed into symmetric and asymmetric terms as $A_{\rm hf}$ = 0.26 + (0.07, -0.05, -0.02) T/$\mu_{\rm B}$. The asymmetric term is explained purely by the direct dipole coupling from the localized Sm spins, which is calculated to be (0.061, -0.053, -0.016) T/$\mu_{\rm B}$ by summing up the dipole fields from Sm moment within 100 Å from the target Be(II) site. This is in contrast with the results for UBe_{13}, where a dipole coupling to the Be p electrons also contribute to the asymmetric hyperfine fields because of the hybridization between Be p electrons with U 5f electrons.[SM1)] A negligibly small p-electron contribution in $SmBe_{13}$ suggests a weak p-f hybridization.

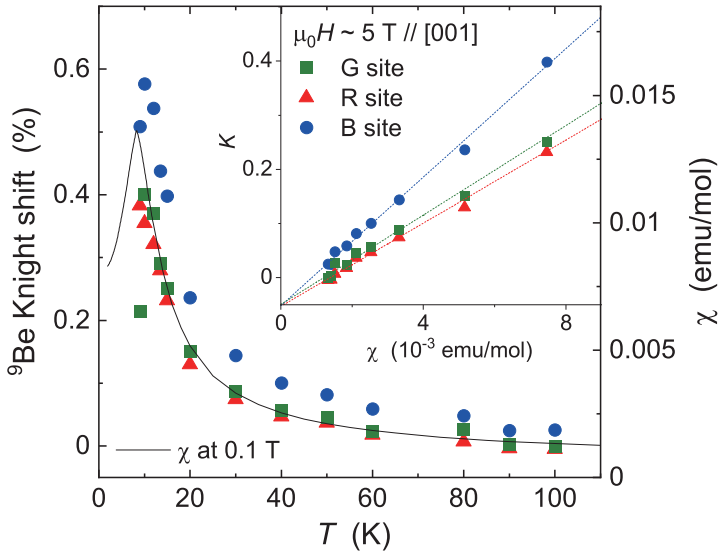

Fig. S2. (Color online) Temperature dependence of Knight shift for three Be(II) sites. Inset shows the K–χ plot for each site.

2. Initial phase dependence of NMR spectra

In the helical magnetic structure, Sm moments are aligned in the helical plane. Such a structure has a freedom of global rotation within the helical plane, which is parameterized by the initial phase ϕ_0 in equations (1)-(3) in the main text. The internal fields at the Be(II) sites change with ϕ_0, and thus the NMR spectral shape has ϕ_0 dependence. In contrast, the bulk magnetization does not depend on this microscopic parameter. We defined that the magnetic structures shown in Fig. 4 correspond to $\phi_0 = 0$. In Fig. S3, we show the spectral shapes for other ϕ_0 calculated for three helical planes of (001), (011), and (111) and two field directions parallel to [001] and [011]. In the case of proper helical [Fig. S3(a)] one spectrum for $\phi_0 = 0$ is shown, as the internal field distribution along the external field direction does not depend on ϕ_0. For other cases, we calculated the spectra for $0^\circ < \phi_0 < 30^\circ$ as the shift in ϕ_0 by 60° gives the identical spectral shape, reflecting the six-fold translational symmetry. Among all these spectra $\phi_0 = 0$ for (111) helical plane fit to the experimental results both in fields along [001] and [011] directions, which leads us to suggest the tilted helical structure as we discussed in the main text.

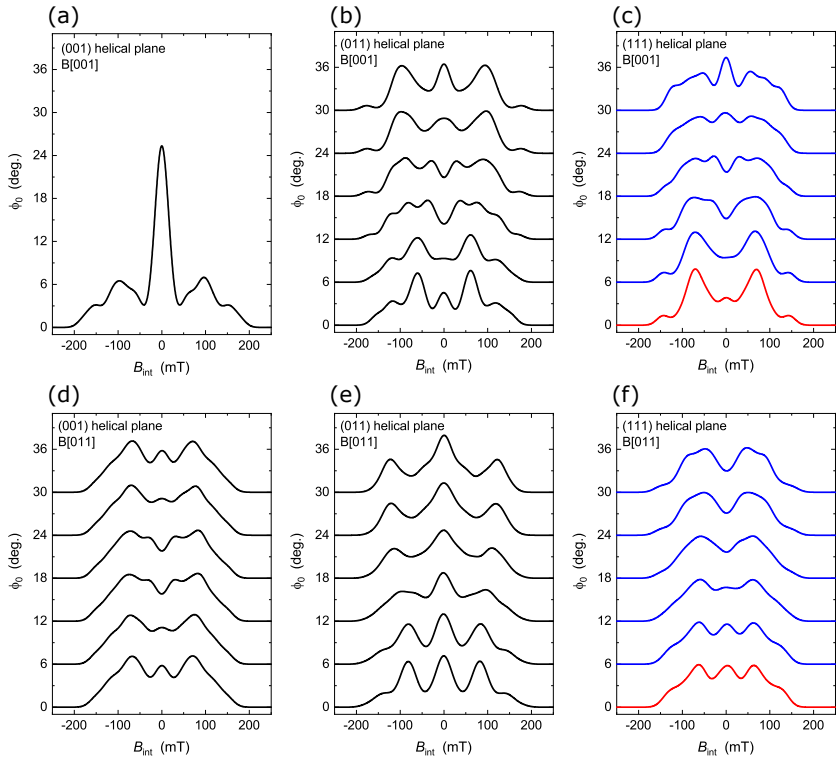

Fig. S3. The ϕ_0 dependence of NMR spectra assuming (a) the (001) helical plane, (b) the (011) helical plane, and (c) the (111) helical plane in magnetic fields applied along the [001] direction, and (d) the (001) helical plane, (e) the (011) helical plane, and (f) the (111) helical plane in magnetic fields applied along the [011] direction. Each spectrum is offset by ϕ_0 for good visibility. Only one spectrum is shown in (a) because no ϕ_0 dependence was found for (001) helical plane in [001] field direction. The two-peak structure in [001] field direction and trapezoidal structure in [011] field direction are obtained at $\phi = 0$ in (111) helical plane.

3. Magnetization based on the CEF model

We show the magnetization of $SmBe_{13}$ calculated based on the crystalline-electric-field (CEF) effect. The magnetization can be calculated by

$$M = g_J \mu_B \sum_n \frac{\langle n| \boldsymbol{J} |n\rangle}{Z} \exp(-E_n/k_B T).$$

Here, $g_J = 2/7$ is the Landé g factor, μ_B is the Bohr magneton, and the total angular momentum $J = 5/2$. The eigenvalue E_n and the eigenfunction $|n\rangle$ were obtained by diagonalizing the total Hamiltonian

$$\begin{aligned} H &= H_{CEF} - g_J \mu_B \boldsymbol{J} \cdot (\mu_0 \boldsymbol{H}) \\ &= W\left[\frac{x}{F(4)}(O_4^0 + 5O_4^4) + \frac{1-|x|}{F(6)}(O_6^0 - 21O_6^4)\right] - g_J \mu_B \boldsymbol{J} \cdot (\mu_0 \boldsymbol{H}). \end{aligned}$$

The first term is the CEF Hamiltonian rewritten by the x and W parameters,[SM2)] and the second term is the Zeeman term.

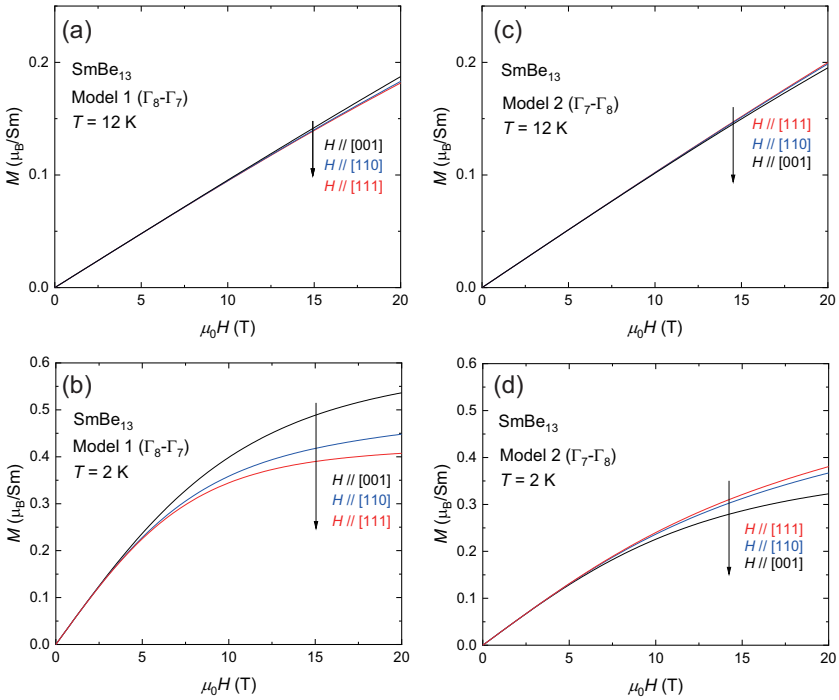

Fig. S4. (Color online) The calculated magnetization process based on the CEF effect for model 1 (Γ_8–Γ_7 with Δ = 90 K) at (a) 12 K and (b) 2 K and for model 2 (Γ_7–Γ_8 with Δ = 30 K) at (c) 12 K and (d) 2 K,

Figures S4 show the calculated magnetization process for the cubic [001], [011], and [111] directions assuming two CEF level scheme models proposed for $SmBe_{13}$ thus far. To investigate the magnetic anisotropy clearly, the calculations were carried out at a lower temperature of 2 K in addition to 12 K, where the effect of the magnetic ordering is excluded. Model 1 is the Γ_8–Γ_7 CEF level scheme with energy separation Δ = 90 K (x = 1 and W = -15 K),[11] and model 2 is the Γ_7–Γ_8 scheme with Δ = 30 K (x = 1 and W = 5 K).[13] The magnetization easy axis determined experimentally is consistent with that parallel to [001] for model 1, not parallel to [111] for model 2. Thus, in terms of magnetic anisotropy, model 1 provides better description of the CEF state of $SmBe_{13}$. Note that the M values for [011] and [111] obtained from the experiments are opposite to the calculated results based on model 1, which might be due to the experimental accuracy. The discrepancy in the value of the horizontal axis between the calculated and the experimental results would be improved by taking the molecular field into consideration.

References

[SM1] H. Tou, N. Tsugawa, M. Sera, H. Harima, Y. Haga, and Y. Ōnuki, J. Phys. Soc. Jpn. **76**, 024705 (2007).

[SM2] K.R. Lea, M.J.M. Leask, and W.P. Wolf, J. Phys. Chem. Solids **23**, 1381 (1962).

[11] H. Hidaka, S. Yamazaki, Y. Shimizu, N. Miura, C. Tabata, T. Yanagisawa, and H. Amitsuka, J. Phys. Soc. Jpn. **86**, 074703 (2017).

[13] M. J. Besnus, P. Panissod, J. P. Kappler, G. Heinrich, and A. Meyer, J. Magn. Magn. Mater. **31–34**, 227 (1983).